A novel two-dimensional organostannoxane coordination network promoted by phenazine: Synthesis, characterization and X-ray structure of $^2_\infty\{[n\text{-Bu}_2(\mu\text{-OH})\text{SnOSn}(\mu\text{-}\eta^2\text{-O}_3\text{SCF}_3)n\text{-Bu}_2]_2[n\text{-Bu}_2(\eta^1\text{-O}_3\text{SCF}_3)\text{SnOSn}(\mu\text{-OH})n\text{-Bu}_2]_2\}$

Laurent Plasseraud *, Hélène Cattey, Philippe Richard, Danielle Ballivet-Tkatchenko

Institut de Chimie Moléculaire de l'Université de Bourgogne (ICMUB), UMR CNRS 5260, UFR Sciences et Techniques, 9 allée A. Savary, BP 47870, F-21078 DIJON Cedex, France

ARTICLE INFO

ABSTRACT

Reaction of the dimeric hydroxo di-*n*-butylstannane trifluoromethanesulfonato complex $[n\text{-Bu}_2\text{Sn}(\mu\text{-OH})(\text{H}_2\text{O})_{0.5}(\eta^1\text{-O}_3\text{SCF}_3)]_2$ (**1**) with phenazine ($\text{C}_{12}\text{H}_8\text{N}_2$, Phz) (**2**) in dichloromethane at room temperature in a 1:3 molar ratio yielded the novel two-dimensional organometallic coordination polymer $^2_\infty\{[n\text{-Bu}_2(\mu\text{-OH})\text{SnOSn}(\mu\text{-}\eta^2\text{-O}_3\text{SCF}_3)n\text{-Bu}_2]_2[n\text{-Bu}_2(\mu\text{-OH})\text{SnOSn}(\eta^1\text{-O}_3\text{SCF}_3)n\text{-Bu}_2]_2\}$ (**3**), together with the phenazinium trifluoromethanesulfonate salt $[\text{C}_{12}\text{H}_9\text{N}_2]^+$ $[\text{CF}_3\text{SO}_3]^-$, crystallographically isolated in two different structural arrangements, free **4** and in π–π aromatic stacking interaction with independent intercalated non-protonated phenazine molecules **5**. Organometallic coordination polymer **3** consists of an infinite one-dimensional chain composed of tetrameric hydroxo tetra-*n*-butyldistannoxane units bridged by bidendate trifluoromethanesulfonate ligands, $(\mu\text{-}\eta^2\text{-O}_3\text{SCF}_3)$. The formation of weak intermolecular interactions between nearest-neighbour chains through the *pseudo*-terminal trifluoromethanesulfonate ligands $(\eta^1\text{-O}_3\text{SCF}_3)$ gives rise to the expansion of an unexpected supramolecular two-dimensional network. The re-crystallisation of **3** in methanol leads to the polymorphic structure $^2_\infty\{[n\text{-Bu}_2(\mu\text{-OH})\text{SnOSn}(\mu\text{-}\eta^2\text{-OSO}_2\text{CF}_3)n\text{-Bu}_2]\}$ (**3b**).

© 2009 Elsevier B.V. All rights reserved.

1. Introduction

The past few years have witnessed an exponentially growing interest in the field of coordination polymers. Basically, their construction is based on the coordination of metal centres by multidentate organic rigid ligands containing donor atoms, in most of cases nitrogen- and oxygen-atoms. Several criteria control the dimensionality of the resulting structures. The most prevalent are the type of organic ligands used, the nature of metal centres, the presence of counter ions and the participation of solvent molecules to the assemblies, giving rise to one-, two- or three-dimensional networks. In addition to coordination bonding, the participation of weak non-covalent interactions in such as hydrogen bonding, π–π contacts, van der Waals and ionic forces, increases tremendously the possibilities of generation and motifs of multidimensional organisations. The choice of the molecular building blocks plays a determinant role for the final properties of the synthesised materials [1–17]. Lately, two well-documented reviews highlighted in particular the engineering and the applications of coordination polymer networks [18,19].

The extension of this methodology to the use of organometallic metal-complexes or metal-clusters as building blocks, instead of simple metal ions can lead to the formation of supramolecular organometallic coordination networks [20–28]. This more recent approach is particularly promising in order to elaborate multidimensional networks with more advanced catalytic and porous properties, taking advantage of the specific properties of define organometallic complexes.

The present contribution reports and describes the preparation of such self-assembly construction based on tin(IV) dinuclear complex used as starting units. In the course of our ongoing studies on chemistry and catalytic properties of di-*n*-butyltin(IV) derivatives [29–32], we isolated the unexpected trifluoromethanesulfonato di-*n*-butyltin(IV)-based supramolecular 2D frame work $^2_\infty\{[n\text{-Bu}_2(\mu\text{-OH})\text{SnOSn}(\mu\text{-}\eta^2\text{-O}_3\text{SCF}_3)n\text{-Bu}_2]_2[n\text{-Bu}_2(\mu\text{-OH})\text{SnOSn}(\eta^1\text{-O}_3\text{SCF}_3)n\text{-Bu}_2]_2\}$ (**3**) from the reaction of the known dinuclear hydroxo complex $[n\text{-Bu}_2\text{Sn}(\mu\text{-OH})(\text{H}_2\text{O})_{0.5}(\eta^1\text{-O}_3\text{SCF}_3)]_2$ (**1**) with molecules of phenazine (Phz) $\text{C}_{12}\text{H}_8\text{N}_2$ (**2**). In the past, Otera and Co-workers have reported a polymorphic structure of **3** characterised as $^2_\infty\{[n\text{-Bu}_2(\mu\text{-OH})\text{SnOSn}(\mu\text{-}\eta^2\text{-O}_3\text{SCF}_3)n\text{-Bu}_2]\}$ (**3b**) and prepared from the direct treatment of two equivalents of *n*-Bu₂SnO with trifluoromethanesulfonic acid in dry acetone [33]. By changing the conditions of our crystallization, compound **3** is converted into Otera's complex **3b**. Herein, we compare the

* Corresponding author. Tel.: +33 3 80 39 38 18; fax: +33 3 80 39 60 98.
  E-mail address: laurent.plasseraud@u-bourgogne.fr (L. Plasseraud).

two-dimensional structural arrangements depicted by each polymorph. In addition, the formation mechanism of **3** is supported by the co-crystallisation of $[C_{12}H_9N_2]^+$ $[CF_3SO_3]^-$, crystallographically isolated in two structural arrangements, free **4** and in π–π aromatic stacking interactions with independent non-protonated phenazine molecules **5**. Finally, we report *in situ* $^{119}Sn\{^1H\}$ NMR spectroscopic measurements carried out to elucidate the formation mechanism of **3**.

2. Experimental

2.1. General

All reactions were carried out under dry argon using Schlenk tube techniques. The organic solvents were refluxed over appropriate dessicants, distilled, and saturated with argon prior to use. Chemicals were purchased from Aldrich and Acros Organics and used without further purification. The starting compound [*n*-Bu$_2$Sn(μ-OH)(H$_2$O)$_{0.5}$(η^1-O$_3$SCF$_3$)]$_2$ was synthesised from *n*-Bu$_2$SnO and trifluoromethanesulfonic acid according to a published method [34]. The ^1H, ^{19}F, $^{119}Sn\{^1H\}$, and $^{13}C\{^1H\}$ NMR experiments were run at 298 K on a Bruker Avance 300 spectrometer at 300.131, 282.404, 111.910, and 75.475 MHz, respectively; and calibrated with Me$_4$Si, trifluoromethylbenzene or Me$_4$Sn as an internal standard. Chemical shift δ values are given in ppm. IR spectra were recorded on a Bruker Vector 22 equipped with a Specac Golden Gate™ ATR device. UV–Vis absorption spectra were recorded on a prim Advanced spectrophotometer 230 V. Elemental analyses (C, H, N, S) were performed at the Institut de Chimie Moléculaire de l'Université de Bourgogne, Dijon.

2.2. Synthesis of $^2_\infty\{[n\text{-}Bu_2(\mu\text{-}OH)SnOSn(\mu\text{-}\eta^2\text{-}O_3SCF_3)n\text{-}Bu_2]_2[n\text{-}Bu_2(\mu\text{-}OH)SnOSn(\eta^1\text{-}O_3SCF_3)n\text{-}Bu_2]_2\}$ (**3**)

Three molar equivalents of phenazine (C$_{12}$H$_8$N$_2$) (0.24 g, 1.32 mmol) were added to a solution of [*n*-Bu$_2$Sn(μ-OH)(H$_2$O)$_{0.5}$(η^1-O$_3$SCF$_3$)]$_2$ (0.37 g, 0.44 mmol) in dichloromethane (25 mL) at 20 °C, and then additional fresh toluene (25 mL) were introduced for crystallisation. After several days, the slow evaporation of the yellow solution afforded colourless square single-crystals characterised as **3** (0.083 g, 29%). ^1H NMR (CD$_2$Cl$_2$): δ 0.98 (t, $^3J_{H-H}$ = 7.4 Hz, 48 H), 1.30–1.90 (m, 96 H); $^{13}C\{^1H\}$ NMR (CD$_2$Cl$_2$): δ 120.6 (CF$_3$, q, $^1J_{C-F}$ = 318 Hz), 27.85, 27.55, 27.51, 27.49, 26.93, 25.75, 14.07 (*n*-butyl C δ), 14.01 (*n*-butyl C δ); $^{119}Sn\{^1H\}$ NMR (CD$_2$Cl$_2$): δ −137.2, −143.9; ^{19}F NMR (CD$_2$Cl$_2$): δ −78.40. IR (cm^{-1}): 3417(br), 2960(m), 2926(m), 2858(m), 1465(m), 1378(w), 1270(m), 1232(s), 1221(s), 1174(s), 1080(m), 1019(s), 879(m), 633(s), 540(s). Anal. Calc. for C$_{68}$H$_{148}$F$_{12}$O$_{20}$S$_4$Sn$_8$: C, 31.51; H, 5.76; S, 4.95. Found: C, 31.42; H, 5.77; S, 4.65%.

2.3. Crystal structure determinations

Colourless squares **3**, yellow squares **4** and red-orange needles **5**, single-crystals were grown successively from the mother-liquor (mixture of dichloromethane/toluene) at room temperature. Colourless needles single-crystals **3b** were obtained by slow evaporation at room temperature of a methanolic solution of compound **3**. Diffraction data were collected from suitable crystals on a Nonius Kappa CCD (Mo Kα radiation, λ = 0.71073 Å) at 115 K for **3**, **3b** and **5** and at 293 K for **4**. The structures were solved using direct methods (SIR 92) [35] and refined with full-matrix least-squares

Table 1
Crystal and structure refinement data for **3**, **3b**, **4**, and **5**.

Compounds	3	3b	4	5
Empirical formula	C$_{34}$H$_{74}$F$_6$O$_{10}$S$_2$Sn$_4$	C$_{34}$H$_{74}$F$_6$O$_{10}$S$_2$Sn$_4$	C$_{13}$H$_9$N$_2$F$_3$O$_3$S	C$_{19}$H$_{13}$N$_3$F$_3$O$_3$S
Formula weight	1295.81	1295.81	330.28	420.39
Temperature (K)	115(2)	115(2)	293(2)	115(2)
Crystal system	Triclinic	Monoclinic	Monoclinic	Triclinic
Space group	$P\bar{1}$	$P2_1/n$	$P2_1/n$	$P\bar{1}$
a (Å)	13.4238(2)	9.652(5)	9.7008(2)	5.8729(1)
b (Å)	14.3843(2)	20.492(5)	14.1690(2)	12.6370(2)
c (Å)	15.0560(2)	25.117(5)	11.2824(4)	13.0867(2)
α (°)	69.621(1)			115.022(1)
β (°)	71.184(1)	90.217(5)	113.213(1)	92.928(1)
γ (°)	77.844(1)			90.796(1)
Volume (Å^3)	2563.73(6)	4980(3)	1425.23(6)	878.26(2)
Z	2	4	4	2
$\rho_{calc.}$ (g/cm^3)	1.679	1.728	1.539	1.590
μ (mm^{-1})	2.073	2.135	0.275	0.244
$F(000)$	1288	2576	672	430
Crystal size (mm^3)	0.45 × 0.45 × 0.15	0.25 × 0.175 × 0.075	0.50 × 0.25 × 0.125	0.47 × 0.30 × 0.20
θ Range (°)	1.50–27.49	2.26–27.49	2.35–27.49	3.13–27.49
Index ranges	h: −17; 17	h: −12; 12	h: −12; 12	h: −7; 7
	k: −18; 18	k: −25; 26	k: −18; 17	k: −16; 16
	l: −19; 19	l: −32; 32	l: −14; 14	l: −16; 16
Reflections collected	21 492	21 769	6138	7379
[$R_{(int)}$]	0.0157	0.0386	0.0239	0.0136
Reflections with $I \geqslant 2\sigma(I)$	10 760	7792	2213	3530
Data/restraints/parameters	11 692/8/522	11 400/0/505	3252/0/199	3980/0/263
Final R indices [$I \geqslant 2\sigma(I)$]	R_1^a = 0.0274	R_1^a = 0.0355	R_1^a = 0.0677	R_1^a = 0.0316
	wR_2^b = 0.0664	wR_2^b = 0.0646	wR_2^b = 0.2017	wR_2^b = 0.0855
R indices (all data)	R_1^a = 0.0309	R_1^a = 0.0731	R_1^a = 0.0973	R_1^a = 0.0369
	wR_2^b = 0.0684	wR_2^b = 0.0747	wR_2^b = 0.2235	wR_2^b = 0.0890
Goodness-of-fit^c on F^2	1.063	1.043	1.088	1.040
Largest difference peak and hole (e Å^{-3})	2.464 and −1.453	0.910 and −0.954	0.606 and −0.379	0.366 and −0.350
CCDC deposition no.	667811	667812	667813	667814

^{a} $R_1 = \Sigma(||F_o| - |F_c||)/\Sigma|F_o|$.
^{b} $wR_2 = [\sum w(F_o^2 - F_c^2)^2 / \sum [w(F_o^2)^2]^{1/2}$, where $w = 1/[\sigma^2(F_o^2 + (0.0284P)^2 + 4.0383P]$ for **3**. $w = 1/[\sigma^2(F_o^2 + (0.0298P)^2 + 1.9432P]$ for **3b**. $w = 1/[\sigma^2(F_o^2 + (0.123P)^2 + 0.5583P]$ for **4** and $w = 1/[\sigma^2(F_o^2 + (0.0468P)2 + 0.2761P]$ for **5**, where $P = (Max(F_o^2.0) + 2 * F_c^2)/3$.
^{c} $S = [\sum w(F_o^2 - F_c^2)^2/(n - p)]^{1/2}$ (n = number of reflections, p = number of parameters).

methods based on F^2 (SHELX-97) [36] with the aid of the WINGX program [37]. All non-hydrogen atoms were refined with anisotropic thermal parameters. Hydrogen atoms were included in their calculated positions and refined with a riding model. In **3**, one of the butyl groups was found disordered over two positions with occupation factors equal to 0.78:0.22. The minor component of the disordered group was isotropically refined and restraints were applied on the Sn–C and C–C distances. Crystallographic data and structures refinement details for **3**, **3b**, **4** and **5** are summarised in Table 1.

3. Results and discussion

3.1. Isolation and spectroscopic characterization of **3**

Air-stable two-dimensional organometallic coordination polymer **3** was prepared in dichloromethane at room temperature together with phenazinium trifluoromethanesulfonate salts, $[C_{12}H_9N_2]^+[CF_3SO_3]^-$ (**4**) and (**5**), by reaction of dimeric trifluoromethanesulfonato hydroxo organotin(IV) $[n\text{-}Bu_2Sn(\mu\text{-}OH)(H_2O)_{0.5}(\eta^1\text{-}O_3SCF_3)]_2$ (**1**) with three molar equivalents of phenazine $(C_{12}H_8N_2, Phz)$ (**2**). Distinct single-crystals of **3**, **4** and **5** suitable for X-ray diffraction studies, colourless squares, yellow squares and red-orange needles, respectively, were successively obtained at room temperature by slow evaporation from a mixture of dichloromethane/toluene.

The $^{119}Sn\{^1H\}$ NMR spectrum in $CDCl_2$ of an analytically pure sample of the starting complex $[n\text{-}Bu_2Sn(\mu\text{-}OH)(H_2O)_{0.5}(\eta^1\text{-}O_3SCF_3)]_2$ (**1**) exhibits only one broad resonance at −151.5 ppm (Fig. 1a). Despite a low solubility in CD_2Cl_2, the $^{119}Sn\{^1H\}$ NMR

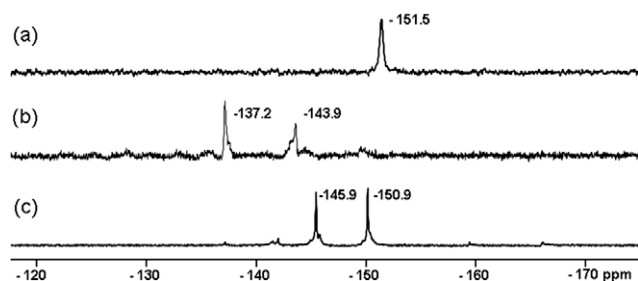**Fig. 1.** $^{119}Sn\{^1H\}$ NMR spectra at 298 K: (a) **1** (CD_2Cl_2), (b) **3** (CD_2Cl_2, slightly soluble), and (c) **3b** (($CD_3)_2CO$).
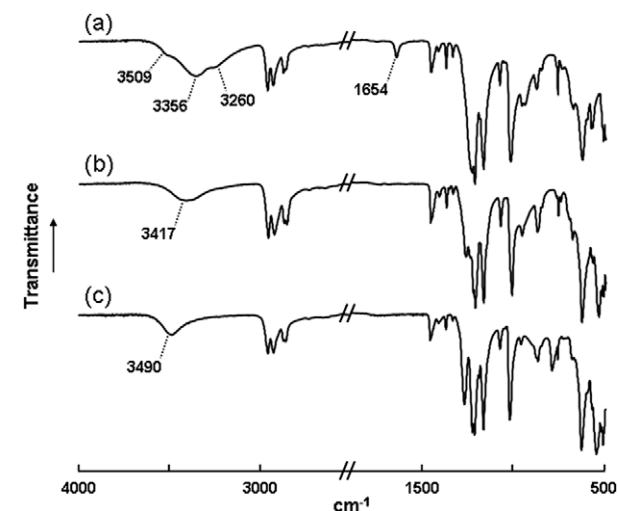

Fig. 2. IR(ATR) spectra: (a) **1**, (b) **3**, and (c) **3b**.

analysis of **3** displays a different pattern revealing one pair of broad signals located at $\delta = -137.2, -143.9$ ppm, and which can be assign to exo- and endocyclic tin nucleus of the tetra-*n*-butyldistannoxane units (Fig. 1b). In the $^{13}C\{^1H\}$NMR spectrum of **3**, two sets of signals are observed for the *n*-butyl groups that it is in agreement with the presence of two different tin sites, while the ^{19}F NMR spectrum exhibits only one singlet situated at −78.40 ppm. The IR spectrum of **3** shows a distinctive broad absorption centred at 3417 cm^{-1}, quite different from the fingerprint of **1** (Fig. 2a), but which can be assigned to the presence of OH groups (Fig. 2b). In addition, the sharp vibration band located at 1654 cm^{-1} on the spectrum of **1** and attributed to the $\delta(HOH)$ bending mode of coordinated water molecule (Fig. 2a), is no longer present in the spectrum of **3** that it implies the displacement of the H_2O-ligands during the reaction with phenazine. Characteristic vibration bands of trifluoromethasulfonate ligands, in particular $\nu(CF_3)$ and $\nu(SO_3)$, are also observed for **3** in the stretching region between 1000 and 1300 cm^{-1} [38]. The micro analytical data confirm as well the composition of **3** (see Section 2).

3.2. Molecular and crystal structures of **3**

Organometallic coordination polymer **3** consists of an infinite one-dimensional chain composed of tetrameric hydroxo tetra-*n*-butyldistannoxane units bridged by bidentate trifluoromethanesulfonate ligands, $(\mu\text{-}\eta^2\text{-}O_3SCF_3)$. All organotin(IV) tetrameric units of **3** adopt a centrosymmetric dimeric structure built up around the planar four-membered cyclic Sn_2O_2 central core and are comparable to a ladder-type arrangement common to many tetraorganodistannoxanes [39]. The dimeric nature of such tetraorganodistannoxanes induces the presence of two distinct tin sites, designated exo- and endocyclic thereafter. Interestingly, the solid-state structure of **3** reveals the presence of two modes of coordination of trifluoromethanesulfonate ligands, bridging and *pseudo*-terminal [40]. Metal coordinated trifluoromethanesulfonate ligands are known to adopt a large diversity of bonding modes, ranging from the ionic, to mono-, bi- or tridentate, terminal or bridging [41]. Numerous examples of trifluoromethanesulfonate derivatives have been reported previously in organotin(IV) chemistry [42,43], displaying in particular excellent Lewis-acid catalytic properties for organic reactions, such as Mukaiyama aldol reaction [44], Robinson annulation [45], acetylation of alcohols [46], and transesterification of dimethyl carbonate with phenol [47]. Lately, we isolated and described the crystallographic structure of the two-dimensional hydroxo di-*n*-butylstannane derivative *catena*-poly[[di-*n*-butyltin(IV)]-μ-trifluoromethanesulfonato-[[di-*n*-butyl(trifluoromethanesulfonato)tin(IV)-di-μ-hydroxo]] combining as well bridging and terminal trifluoromethanesulfonate ligands [48]. In compound **3**, the both modes of coordination of trifluoromethanesulfonate ligands involve a differentiation between the tetrameric tin(IV) units. Firstly, we can distinguish the units connected to two bridging trifluoromethanesulfonate groups and then
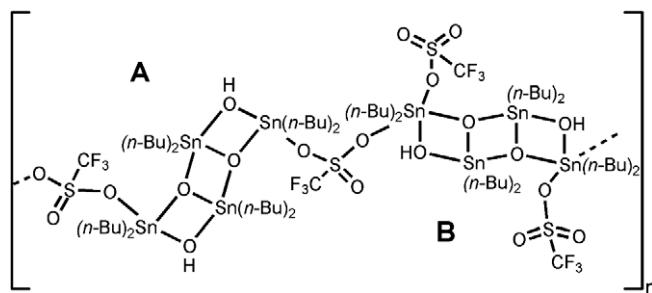
Scheme 1. Schematic representation of the repeating motif of polymer **3**.

the units possessing two *pseudo*-terminal trifluoromethanesulfonate groups, depicted **A** and **B** in Scheme 1, respectively. Both types of tetrameric units, **A** and **B**, are bounded by the bidendate bridging trifluoromethanesulfonate ligands giving rise to an eight tin atoms-based organometallic fragment which constitutes the repeating basic motif of the organometallic polymer **3** (Scheme 1).

An ORTEP view is shown in Fig. 3 and selected bond distances and angles for **3** are listed in Table 2. Each exocyclic Sn1 and Sn1ii atom of unit **A** is six-coordinated. The most suitable description for the coordination geometry can be exposed as an unusual face-capped trigonal bipyramid environment. The axial positions are occupied by the oxygen atom O5 (μ-η^2-O$_3$SCF$_3$) and O1 (μ-OH) [O1–Sn1–O5 = 149.41(7)°, Sn1–O5 = 2.505(2) Å and Sn1–O1 = 2.068(2) Å]. The equatorial plane contains both α-carbon atoms of *n*-butyl chains [C3–Sn1–C7 = 128.34(12)°, Sn1–C3 = 2.138(3) Å and Sn1–C7 = 2.131(3) Å] and the triply bridging oxygen atom O2 [O2–Sn1–C3 = 117.01(10)°, O2–Sn1–C7 = 111.07(10)°, and Sn1–O2 = 2.027(2) Å]. One face of the trigonal bipyramid is capped by an oxygen atom of a terminal trifluoromethanesulfonate ligand (O9v) of a unit **B** from a neighbouring polymeric chain with a long Sn–O bond [Sn1–O9v = 3.067(2) Å] (Fig. 4a). In previous studies on organotin(IV) derivatives, we already reported such similar long Sn–O distances for carbonato and trifluoromethanesulfonato tin(IV) derivatives, which were considered as weak interactions [32,47]. The distortion observed for the axial bond Sn1–O1 can be explained by the capping O9v-oxygen atom [O1–Sn1–O2 = 74.95(7)°, O1–Sn1–C3 = 106.59(11)°, O1–Sn1–C7 = 102.90(10)°]. The endocyclic Sn2 and Sn2ii tin atoms of units **A** are pentacoordinated in a distorted trigonal bipyramidal arrangement (TBP). The equatorial plane contains both α-carbon atoms of *n*-butyl chains [C11–Sn2–C15 = 132.30(20)°, Sn2–C11 = 2.121(3) Å and Sn2–C15 = 2.143(5) Å] and the triply bridging oxygen atom O2 [O2–Sn2–C15 = 113.40(20)°, O2–Sn2–C11 = 114.15(10)°, and Sn2–O2 = 2.064(2) Å]. The axial positions are occupied by the oxygen atoms O1 (μ-OH) and O2ii (μ_3-O) with bond angles smaller than 180°: [O1–Sn2–O2ii = 145.23(7)° Sn2–O1 = 2.191(2) Å and Sn2–O2ii = 2.126(2) Å]. Up to now, to our knowledge, the presence of two different coordination geometries for the endo- and exocyclic sites of organodistannoxane frameworks has been relatively rarely observed. However, a comparable description was reported by Cao and Co-workers for a dimeric dicarboxylato distannoxane derivative in which endo- and exocyclic tin atoms adopt also a distinct five- and six-coordination [49].
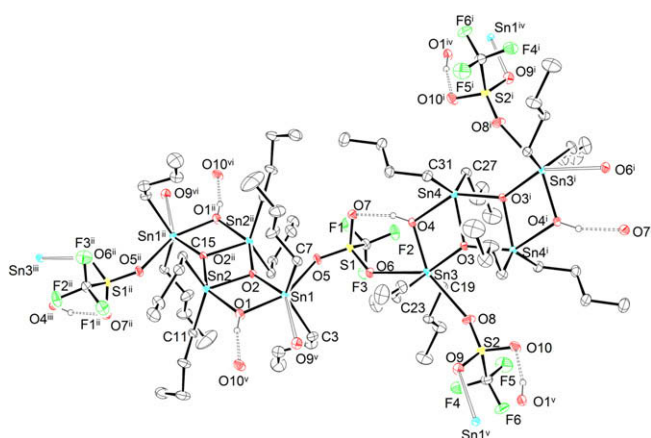
Table 2
Selected bond distances (Å) and angles (°) for **3**.

Sn1–O1	2.068(2)	Sn3–O3	2.031(2)
Sn1–O2	2.027(2)	Sn3–O4	2.069(2)
Sn1–O5	2.505(2)	Sn3–O6	2.763(2)
Sn1–O9	3.067(2)	Sn3–O8	2.564(2)
Sn1–C3	2.138(3)	Sn3–C19	2.123(3)
Sn1–C7	2.131(3)	Sn3–C23	2.123(3)
Sn2–O1	2.191(2)	Sn4–O3	2.063(2)
Sn2–O2	2.064(2)	Sn4–O3i	2.122(2)
Sn2–O2ii	2.126(2)	Sn4–O4	2.217(2)
Sn2–C11	2.121(3)	Sn4–C27	2.130(3)
Sn2–C15	2.143(5)	Sn4–C31	2.127(3)
Sn1–O1–Sn2	103.58(8)	Sn3–O3–Sn4	110.31(8)
Sn1–O2–Sn2	109.79(8)	Sn3–O3–Sn4i	143.91(9)
Sn1–O2–Sn2ii	143.77(9)	Sn3–O4–Sn4	103.24(8)
Sn2–O2–Sn2ii	106.41(8)	Sn4–O3–Sn4i	105.58(7)
O1–Sn1–O2	74.95(7)	O3–Sn3–O4	75.06(7)
O1–Sn1–O5	149.41(7)	O3–Sn3–C19	108.91(9)
O1–Sn1–C3	106.59(11)	O3–Sn3–C23	111.10(10)
O1–Sn1–C7	102.90(10)	O4–Sn3–O8	152.10(8)
O2–Sn1–O5	74.45(7)	O4–Sn3–C19	108.68(9)
O2–Sn1–C3	117.01(10)	O4–Sn3–C23	104.98(11)
O2–Sn1–C7	111.07(10)	C19–Sn3–C23	132.79(11)
O5–Sn1–C3	87.12(10)	O3–Sn4–O3i	74.42(7)
O5–Sn1–C7	88.38(9)	O3–Sn4–O4	71.31(7)
C3–Sn1–C7	128.34(12)	O3–Sn4–C27	112.87(10)
O1–Sn2–O2	71.63(7)	O3–Sn4–C31	111.80(10)
O1–Sn2–O2ii	145.23(7)	O3i–Sn4–O4	145.70(7)
O1–Sn2–C11	95.41(10)	O3i–Sn4–C27	100.55(10)
O1–Sn2–C15	96.23(16)	O3i–Sn4–C31	98.43(9)
O2–Sn2–O2ii	73.59(8)	O4–Sn4–C27	91.30(9)
O2–Sn2–C11	114.15(10)	O4–Sn4–C31	95.59(10)
O2–Sn2–C15	113.40(20)	C27–Sn4–C31	134.64(12)
O2ii–Sn2–C15	97.66(17)		
O2ii–Sn2–C11	98.43(10)	S1–O5–Sn1	124.19(11)
C11–Sn2–C15	132.30(20)		

Symmetry transformations used to generate equivalent atoms: (i) $1 - x$, $1 - y$, $1 - z$; (ii) $-x$, $2 - y$, $-z$.

In the unit **B** of **3**, the coordination geometry of tin centres is similar to the unit **A**. Indeed, the exocyclic Sn3 and Sn3i atoms are bonded to two *n*-butyl groups and to four types of oxygen atoms (μ_3-O, μ-OH, μ-η^2-O$_3$SCF$_3$, and η^1-O$_3$SCF$_3$). The coordination can be also regarded as being a face-capped trigonal bipyramid geometry with the oxygen atoms O4 (μ-OH) and O8 (η^1-O$_3$SCF$_3$) occupying the axial positions [O4–Sn3–O8 = 152.10(8)°, Sn3–O4 = 2.069(2) Å and Sn3–O8 = 2.564(2) Å]. The equatorial plane contains both α-carbon atoms of *n*-butyl chains [C19–Sn3–C23 = 132.79(11)°, Sn3–C19 = 2.123(3) Å and Sn3–C23 = 2.123(3) Å] and the triply bridging oxygen atom O3 [O3–Sn3–C19 = 108.91(9)°, O3–Sn3–C23 = 111.10(10)°, and Sn3–O3 = 2.031(2) Å]. One face of the trigonal bipyramid is capped by an
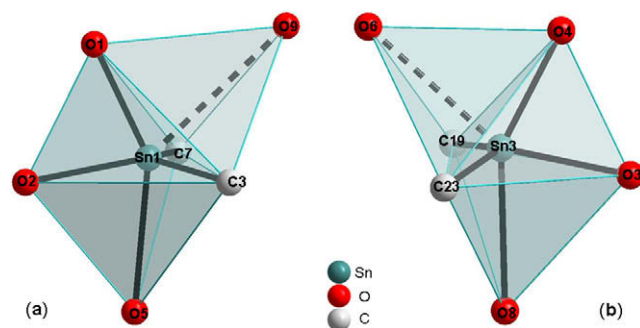

Fig. 3. Molecular structure of the repeating motif of **3** showing the atom labelling scheme (ORTEP view). Colour code: tin, turquoise; sulphur, yellow; oxygen, red; fluoride, green; carbon, grey. Symmetry transformations used to generate equivalent atoms: (i) $1 - x$, $1 - y$, $1 - z$; (ii) $-x$, $2 - y$, $-z$; (iii) $-x$, $2 - y$, $-z$; (iv) $1 + x$, y, z; (v) $-x$, $1 - y$, $1 - z$; (vi) x, $1 + y$, $z - 1$. (For interpretation of the references to colour in this figure legend, the reader is referred to the web version of this article.)

Fig. 4. The coordination environment around the Sn1 (a) and Sn3 (b) tin centres highlighting unusual distorted capped trigonal bipyramid geometry (DIAMOND presentation).

oxygen atom of a bridging trifluoromethanesulfonate ligand (O6) with a distance shorter than in unit **A** [Sn3–O6 = 2.763(2) Å] (Fig. 4b). Again, the distortion observed for the axial bond Sn3–O4 can be explained by the capping O6-oxygen atom [O3–Sn3–O4 = 75.06(7)°, O4–Sn3–C19 = 108.68(9)°, O4–Sn3–C23 = 104.98(11)°]. The endocyclic Sn4 and Sn4^i atoms are pentacoordinated in a distorted trigonal bipyramidal arrangement (TBP). The equatorial plane contains both *n*-butyl groups [C27–Sn4–C31 = 134.64(12)°, Sn4–C27 = 2.130(3) Å and Sn4–C31 = 2.127(3) Å] and
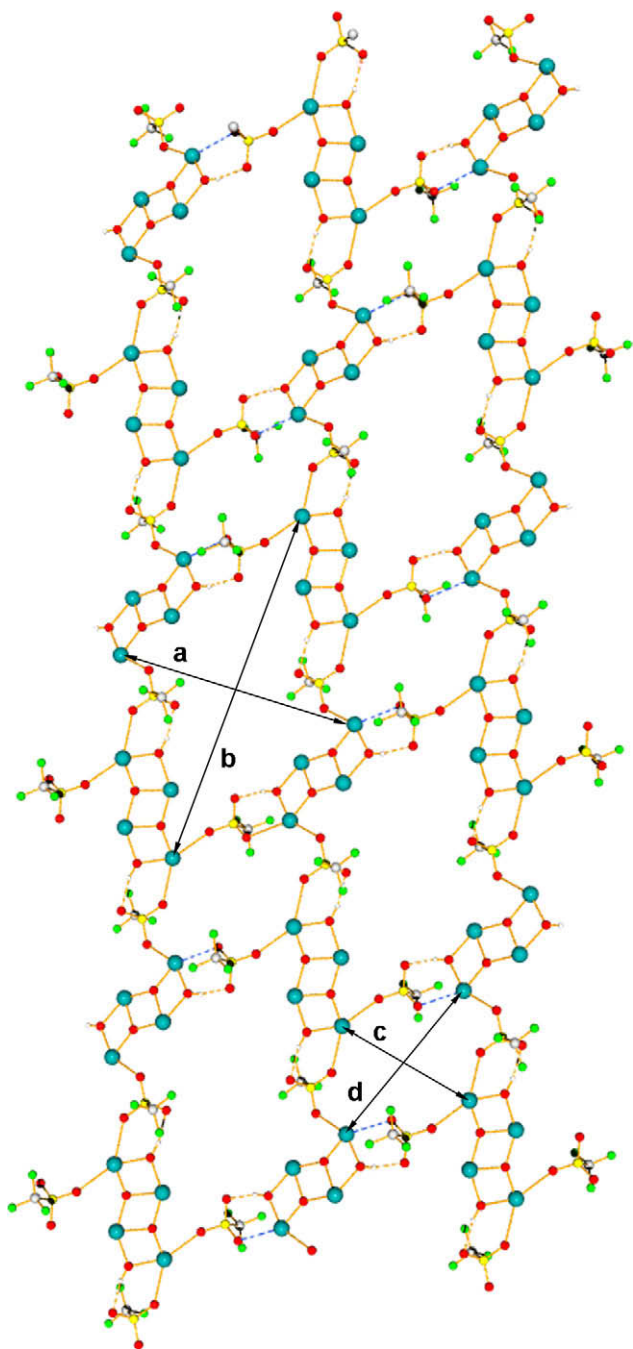
the triply bridging atom O3 (μ_3-O) [O3–Sn4–C27 = 112.87(10), O3–Sn4–C31 = 111.80(10)°, and Sn4–O3 = 2.063(2) Å]. The axial positions are occupied by the oxygen atoms O4 (μ-OH) and O3^i (μ_3-O) with bond angles smaller than 180°: [O3^i–Sn4–O4 = 145.70(7)° Sn4–O4 = 2.217(2) Å and Sn4–O3^i = 2.122(2) Å].

The uncoordinated oxygen atom of the bridging trifluoromethanesulfonate ligand is involved in an intramolecular hydrogen bonding interaction with a bridging hydroxo group from a unit **B**, O7⋯(H)O4 [2.868(3) Å]. The uncoordinated oxygen atoms of both *pseudo*-terminal trifluoromethanesulfonate ligand are implicated in intermolecular hydrogen bonding and in long Sn–O distance interaction with one bridging hydroxo group O10⋯(H)O1^v [2.759(2) Å], and with an exocyclic tin atom, Sn1⋯O9^v [3.067(2) Å], respectively, of a unit **A** from the nearest-neighbour infinite chain. The extension of a two-dimensional network containing 32-membered (8Sn, 16O, 4S, 4H) and 16-membered (4Sn, 8O, 4S) macrocycles, results from these weak interactions. The structural arrangement can be compared to a brick wall-like structure constituted of two-size blocks alternatively assembled. A DIAMOND representation is presented in Fig. 5 showing the macrocycle dimensions. Up to now, few solid-state reports of organostannoxane-based supramolecular architectures with large internal cavities have been reported [50–53], but the current growing interest in the construction of metal–organic frameworks (MOFs) arouses more attention to such molecular organotin(IV)-based assemblies. The two-dimensional coordination polymer **3**, $^2_\infty\{[n\text{-Bu}_2(\mu\text{-OH})\text{SnOSn} \ (\mu\text{-}\eta^2\text{-O}_3\text{SCF}_3)n\text{-Bu}_2]_2[n\text{-Bu}_2(\mu\text{-OH})\text{SnOSn} \ (\eta^1\text{-O}_3\text{SCF}_3)n\text{-Bu}_2]_2\}$, constitutes a remarkable example of this fascinating class of construction.

3.3. Conversion of **3** into polymorphic structure **3b**

Chemically, the organometallic polymer **3** is well-soluble in acetone and methanol. However, the solution ^{119}Sn NMR in acetone-d_6, at room temperature, exhibits only one major pair of signals with chemical shifts at δ −145.9 and −150.9 ppm suggesting a structural or a chemical modification of **3** (Fig. 1c). The re-crystallisation in methanol gives rise effectively after few days, to the
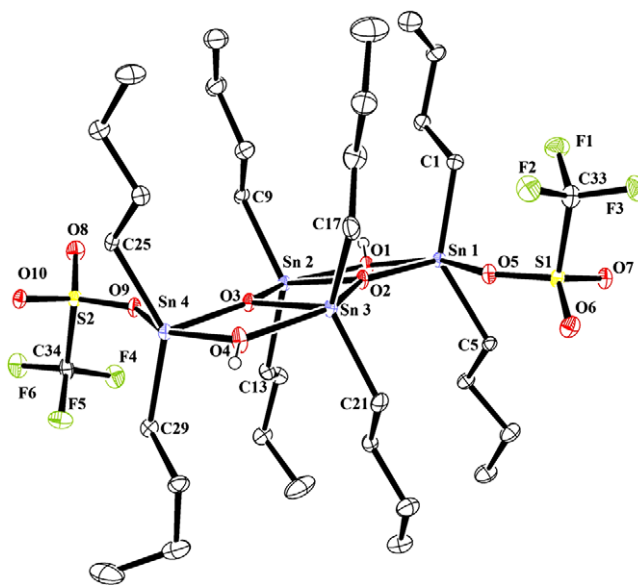

Fig. 5. The two-dimensional supramolecular assembly of **3** (DIAMOND presentation) exhibiting the diagonal dimensions of 32-membered and 16-membered macrocyclic cavities ($a = 13.97$ Å, $b = 20.75$ Å, $c = 8.55$ Å, $d = 10.32$ Å). Hydrogen bonding and long Sn–O distance interactions are shown by orange (O–H⋯O) and blue (Sn⋯O) dashed lines, respectively. *n*-Butyl chains are omitted for clarity. (For interpretation of the references to colour in this figure legend, the reader is referred to the web version of this article.)

Fig. 6. ORTEP representation of the structure of **3b** showing the atom labelling scheme. Colour code: tin, turquoise; sulphur, yellow; oxygen, red; fluoride, green; carbon, grey. Hydrogen atoms of *n*-Butyl chains are omitted for clarity. (For interpretation of the references to colour in this figure legend, the reader is referred to the web version of this article.)

formation of colourless needle-like single-crystals, suitable for an X-ray crystallographic analysis but with a different shape from **3** (squares). The infrared analysis on new crystals confirmed this observation showing a ν(OH) band at 3490 cm^{-1}, narrower and shifted compared to that of **3** (Fig. 2c). Indeed, the structural determination highlighted the presence of a polymorphic structure of **3**, resolved as being $^2_\infty\{[n\text{-Bu}_2(\mu\text{-OH})\text{SnOSn}(\mu\text{-}\eta^2\text{-O}_3\text{SCF}_3)n\text{-Bu}_2]\}$ and annotated thereafter **3b**. An ORTEP view is shown in Fig. 6. In the past, the X-ray crystallographic structure of **3b** was already reported by Otera and Co-workers and was described as tetrameric hydroxo tetra-n-butyldistannoxane units bridged by trifluoromethanesulfonate ligands, giving rise to a sheet-like structure formed of 24-membered rings (CCDC No. 143838) [54]. Carrying out the measurements at lower temperature than Otera's data set, 115 K, and after several attempts, we could collect high-quality crystallographic data involving a better resolution of the structure. Thus, the disorder of some methyl residues in the butyl groups, initially observed by Otera, was clearly refined. It appeared judicious and profitable from a crystallographic point of view to re-actualise in this paper the new crystal and structure refinement data for compound **3b** (included in Table 1, selected bond distances and angles are listed in Table 3). Furthermore, the ^{1}H, ^{13}C{^{1}H} and ^{119}Sn{^{1}H} NMR spectroscopic data measured for **3b** remain identical with what Otera published for this compound [33,54]. In fact, the structures of polymorphs **3** and **3b** differ only in the coordination mode of the trifluoromethanesulfonate ligands, bridging and *pseudo*-terminal for **3** (triclinic), whereas strictly bridging for **3b** (monoclinic). In the case of **3**, both uncoordinated oxygen atoms of *pseudo*-terminal trifluoromethanesulfonate groups support the growth of intermolecular hydrogen bonding and long Sn–O distance interactions described herein, while such weak interactions are not observed for the structure of **3b**. These polymorphic modifications lead to the arrangement of two distinct two-dimensional frameworks shown in Figs. 5 and 7. The update of structures **3** and **3b** represents a novel example of organometallic polymorphism. This concept and in particular the role of weak intermolecular

interactions for such modification were first discussed in detail by Braga and Grepioni in 2000 [55], and then re-examined more recently in 2006 by the same authors [56].

3.4. Molecular and crystal structures of **4** and **5**

As mentioned in the introduction, following the crystallisation of **3**, two new types of coloured crystals were grown successively from the mother-liquor, yellow squares and red-orange needles, and were characterised by X-ray diffraction studies as salts **4** and **5**, respectively. The molecular structure of **4** can be described as constituted by a phenazinium cation, $[\text{C}_{12}\text{H}_9\text{N}_2]^+$, whose only one nitrogen atom is protonated, and by a trifluoromethanesulfonate anion $[\text{CF}_3\text{SO}_3]^-$ in intramolecular hydrogen bonding interaction with the NH group of the cation, O1$\cdots$(H)N1 [2.736(3) Å]. An ortep representation of salt **4** is shown in Fig. 8a. The existence of an orthogonal intermolecular electrostatic contact between a second oxygen atom and the neighbouring phenazinium cation, [O2$\cdots$centroid(C$_4$N$_2$) = 2.746(3) Å] [57], leads to the formation of an infinite one-dimensional assemblage characterised as a split stair chain. The dihedral angle between two consecutive phenazinium-based planes of **4** is 83.52(4)°. The same type of arrangement was previously observed by Munakata and Co-workers for the phenazine-based copper(I) complex $[\{\text{Cu}_2(\mu\text{-I})_2(\mu\text{-phz})\}_\infty]$ [58]. In addition to intramolecular hydrogen bonding and electrostatic contacts, π–π interactions between two aromatic rings of phenazinium of two close infinite chains assemble a supramolecular three-dimensional network. The crystal packing of **4** in the unit cell is reported Fig. 8b. The interplanar and the centroid-to-centroid distances are 3.47(1) and 3.72 Å, respectively. The difference in these two distances indicates that the phenazine and phenazinium rings are slipped. The slip angle (angle between the normal to the planes

Table 3
Selected bond distances (Å) and angles (°) for **3b**.

|			
Sn1–O1	2.071(3)	Sn3–O2	2.109(2)
Sn1–O2	2.043(2)	Sn3–O3	2.052(2)
Sn1–O5	2.600(2)	Sn3–O4	2.234(3)
Sn1–C1	2.122(3)	Sn3–C17	2.128(4)
Sn1–C5	2.126(3)	Sn3–C21	2.138(3)
Sn2–O1	2.243(2)	Sn4–O3	2.044(2)
Sn2–O2	2.060(2)	Sn4–O4	2.050(3)
Sn2–O3	2.113(2)	Sn4–O9	2.668(2)
Sn2–C9	2.131(3)	Sn4–C25	2.125(3)
Sn2–C13	2.126(3)	Sn4–C29	2.113(4)
Sn1–O1–Sn2	101.85(10)	O2–Sn2–C13	114.53(12)
Sn1–O2–Sn2	109.52(11)	O3–Sn2–C9	100.09(12)
Sn1–O2–Sn3	144.24(12)	O3–Sn2–C13	98.13(12)
Sn2–O2–Sn3	105.90(11)	C9–Sn2–C13	131.07(15)
Sn2–O3–Sn3	106.06(11)	O2–Sn3–O3	73.90(10)
Sn3–O3–Sn4	110.36(10)	O2–Sn3–O4	144.93(9)
Sn4–O3–Sn2	142.60(12)	O2–Sn3–C17	108.90(13)
Sn3–O4–Sn4	103.36(10)	O2–Sn3–C21	98.53(12)
O1–Sn1–C1	106.08(12)	O3–Sn3–O4	71.11(9)
O1–Sn1–C5	104.27(12)	O3–Sn3–C17	119.40(13)
O2–Sn1–O1	76.31(9)	O3–Sn3–C21	116.99(12)
O2–Sn1–C1	103.49(12)	O4–Sn3–C17	90.39(14)
O2–Sn1–C5	107.99(12)	O4–Sn3–C21	95.20(13)
C1–Sn1–C5	140.38(14)	C17–Sn3–C21	121.94(15)
O1–Sn2–O2	72.25(9)	O3–Sn4–O4	75.15(9)
O1–Sn2–O3	145.85(9)	O3–Sn4–C25	104.59(12)
O1–Sn2–C9	95.26(12)	O3–Sn4–C29	104.39(12)
O1–Sn2–C13	94.31(12)	O4–Sn4–C25	106.98(12)
O2–Sn2–O3	73.65(10)	O4–Sn4–C29	105.79(12)
O2–Sn2–C9	114.10(12)	C29–Sn4–C25	140.63(14)
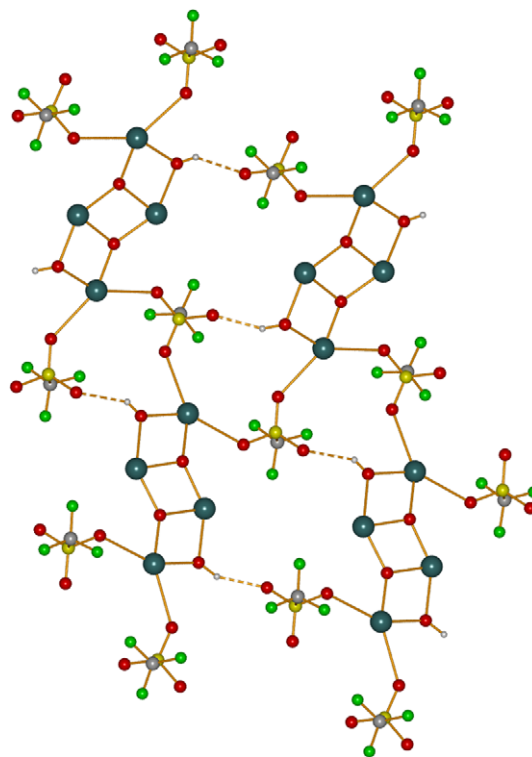
Fig. 7. The two-dimensional supramolecular assembly of the polymorph compound **3b** (DIAMOND presentation). Colour code: tin, turquoise; sulphur, yellow; oxygen, red; fluoride, green; carbon, grey. n-Butyl chains are omitted for clarity. (For interpretation of the references to colour in this figure legend, the reader is referred to the web version of this article.)
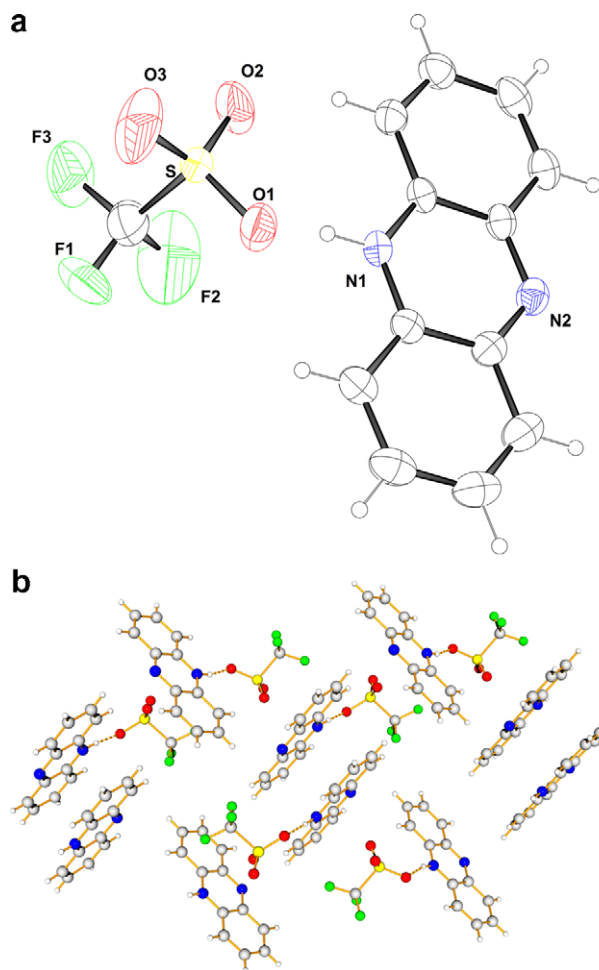
Fig. 8. (a) Molecular structure of $[C_{12}H_9N_2]^+[CF_3SO_3]^-$ (**4**) showing the atom labelling scheme (ORTEP view). Colour code: sulphur, yellow; oxygen, red; nitrogen, blue; fluoride, green; carbon, grey; hydrogen, white. (b) The crystal packing of **4** in the unit cell. Hydrogen bonding interactions (N–H···O) are shown by orange dashed lines (DIAMOND presentation). (For interpretation of the references to colour in this figure legend, the reader is referred to the web version of this article.)

Fig. 9. UV–Vis absorption spectra of **4**, **5** and phenazine (Phz) in CH_2Cl_2 solution ($c = 0.5 \times 10^{-4}$ mol L^{-1}) at 298 K.

Fig. 10. (a) Molecular structure of $\{([C_{12}H_9N_2]^+[CF_3SO_3]^-)_2(C_{12}H_8N_2)\}$ (**5**) showing the atom labelling scheme (ortep view). Colour code: sulphur, yellow; oxygen, red; nitrogen, blue; fluoride, green; carbon, grey; hydrogen, white. (b) The crystal packing of **5** in the unit cell (DIAMOND presentation). Symmetry transformations used to generate equivalent atoms: (i) $-x$, $1-y$, $1-z$. (For interpretation of the references to colour in this figure legend, the reader is referred to the web version of this article.)

and the centroid–centroid vector) is 21° corresponding to a slippage distance of 1.34 Å. For such interactions, the distance between the arene planes is commonly found around 3.3–3.8 Å [59,60]. Comparable interchain π–π interactions were recently reported by Lachgar and Co-workers for the one-dimensional coordination polymer $^1_\infty[Cu(CN)_2(bpy)]$ (bpy = 2,2-bipyridy) [61].

The micro analytical data confirm as well the composition of **4**. Anal. Calc. for $C_{13}H_9N_2F_3O_3S$: C, 47.27; H, 2.75; N, 8.48; S, 9.71. Found: C, 47.33; H, 2.34; N, 8.67; S, 9.77%. The UV–Vis spectrum of **4** in dichloromethane solution displays an intense band at 380 nm while in the same conditions, the free phenazine presents a maximum of absorption at 362 nm which is due to $\pi \leftrightarrow \pi^*$ transition [62](Fig. 9).

The structure of salt **5**, $\{([C_{12}H_9N_2]^+ [CF_3SO_3]^-)_2(C_{12}H_8N_2)\}$, differs from that of **4** by the intercalation of a neutral molecule of phenazine between two phenazinium trifluoromethanesulfonate salt molecules (Fig. 10a). This intercalated molecule is located in a symmetry centre. The sandwich structure of **5** results from slipped π–π aromatic interactions between the three phenazine-type rings. In this interaction, the average interplanar distance between the aromatic rings is 3.32(1) Å, slightly shorter than for salt **4**. The two rings are slipped by 1.36 Å (slip angle equal to 26.44°) and the ring-centroid to ring-centroid distance is 3.708 Å. Analogously to **4**, one of the oxygen atoms of the trifluoromethanesulfo-
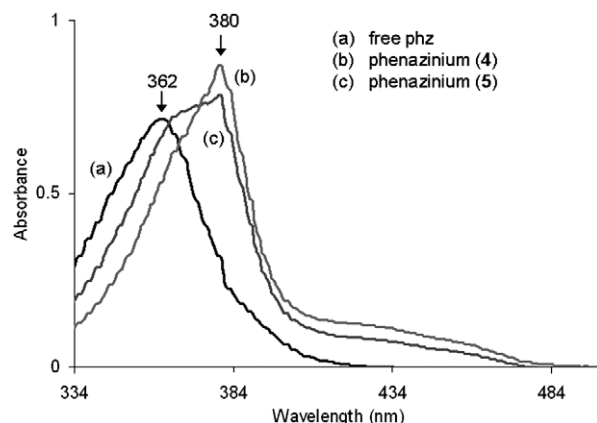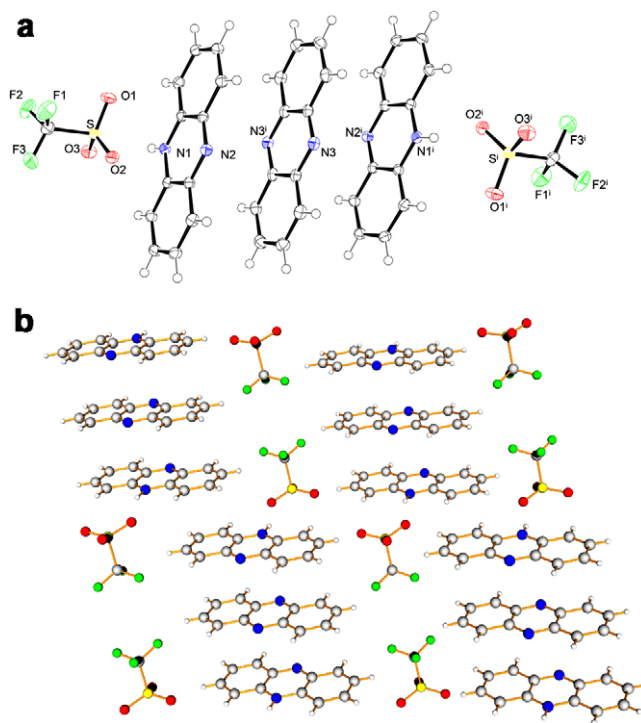
nate anions is engaged in an intermolecular hydrogen bonding interaction with the NH function of a phenazinium cation, O2···(H)N1 [2.704(2) Å]. Additionally, short intramolecular contacts exist also between fluorine and oxygen atoms of trifluoromethanesulfonate anions and the nearest-neighbour molecules of phenazine and phenazinium, through O···(H)C and F···(H)C interactions, and making possible the formation of a three-dimensional network. The crystal packing of **5** in the unit cell is reported in Fig. 10b (DIAMOND representation). The origin of the neutral molecule of phenazine intercalated between both phenazinium molecules can be explained by the initial addition of an excess of phenazine compared to the stoichiometric quantity necessary for

the synthesis of the coordination polymer **3**. The micro analytical data are in agreement with the sandwich formulation of **5**. Anal. Calc. for $\{C_{13}H_9N_2F_3O_3S \cdot \frac{1}{2}(C_{12}H_8N_2)\}$: C, 54.28; H, 3.12; N, 10.00; S, 7.63. Found: C, 53.80; H, 2.83; N, 10.57; S, 7.43%. In addition, the UV–Vis absorption spectrum in dichloromethane confirms undoubtedly that the phenazinium salt **5** results from the combination of $\{[C_{12}H_9N_2]^+[CF_3SO_3]^-\}$ (**4**) and free phenazine ($C_{12}H_8N_2$) (Fig. 9).

Up to now, several self-assembly architectures based on phenazine molecules as well as phenazinium cations have been already indexed in the literature, underlining the predisposition of such N-heterocyclic molecule to generate π–π stacking and hydrogen bonding interactions [63–67]. The reported X-ray crystallographic structures of the phenazinium trifluoromethanesulfonate salt $[C_{12}H_9N_2]^+[CF_3SO_3]^-$, **4** and **5**, are unprecedented and constitute new examples of 3D self-assembly phenazine- and phenazinium-based edifices.

3.5. Mechanistic considerations

While our work was in progress, Chandrasekhar and Co-workers have reported a comparable reaction based on the hydrolysis of the hydrated organotin salt $\{[n\text{-}Bu_2Sn(\mu\text{-}OH_2)_4]^{2+}[2,5\text{-}Me_2C_6H_3SO_3^-]_2\}$ by a nonchelating pyridine molecule affording the co-formation of the polymer $\{[n\text{-}Bu_2Sn(\mu\text{-}OH)(\mu\text{-}\eta^2\text{-}O_3SC_6H_3\text{-}2,5\text{-}Me_2)]_2\}_n$ and the pyridium sulfonate [68]. The mechanism proposed by the authors postulates that pyridine abstracts a proton to afford a tin monohydroxide key-intermediate. In our target reaction, N-heterocyclic phenazine molecules seem to play a similar role extracting a proton from **1** to provide the phenazinium cation, $[C_{12}H_9N_2]^+$, and initiating the formation and the polymerisation of **3**. Both solid-state structures of phenazinium trifluoromethanesulfonate salts reported in this paper, **4** and **5**, constitute undoubtedly experimental clues. A few years ago, we described a comparable reaction for the synthesis of a copper(I) coordination polymer from a discrete dinuclear complex, underlining the role of a bidentate diphenylphosphine as initiator of the polymerisation process [69].

In order to get more data on the mechanism leading to the formation of **3** and to detect intermediate species, we monitored by *in situ* $^{119}Sn\{^1H\}$ NMR spectroscopy, in CD$_2$Cl$_2$ solution, the reactivity of complex $[n\text{-}Bu_2Sn(\mu\text{-}OH)(H_2O)_{0.5}(\eta^1\text{-}O_3SCF_3)]_2$ (**1**) with increasing molar ratio of phenazine **2**. The $^{119}Sn\{^1H\}$ NMR spectrum of an equimolar mixture of **1** and **2** displays three new resonances located at $\delta = -128.3$, -146.9 and -166.5 ppm (Fig. 11a) while the signal assigned to the starting complex **1** ($\delta = -151.5$ ppm, Fig. 1a) is already no longer visible. The addition of two supplementary molar equivalents of **2** leads to the complete disappearance of the more upfield resonance and shows exclusively two signals at $\delta = -128.7$ and -148.8 ppm (relative integration 1:2) which present close chemical shifts to the ones of the previous spectrum (Fig. 11b). This experiment replicates strictly the conditions of the initial reaction carried out in the Schlenk tube and conducting to the crystals of **3**. In the presence of a large excess of phenazine (6 molar equivalents), the preceding $^{119}Sn\{^1H\}$ NMR fingerprint is preserved still exhibiting both the signals at $\delta = -129.0$ and -148.7 ppm with a 1:2 ratio (relative integration), respectively (Fig. 11c). On the basis of such a pattern which differs from **3** ($\delta = -137.2$, -143.9 ppm, Fig. 1b), and from examples described previously in the literature [70,71], we assign these signals to a trinuclear species with two different tin environments. This compound observed in *in situ* conditions constitutes indubitably a key-intermediate for the synthesis of $^2_\infty\{[n\text{-}Bu_2(\mu\text{-}OH)SnOSn(\mu\text{-}\eta^2\text{-}O_3SCF_3)n\text{-}Bu_2]_2[n\text{-}Bu_2(\mu\text{-}OH)SnOSn(\eta^1\text{-}O_3SCF_3)n\text{-}Bu_2]_2\}$ (**3**) from **1** and **2**. Further investigations are in progress to obtain more structural details on this intermediate and to clarify its precise role in the mechanism formation of **3**.
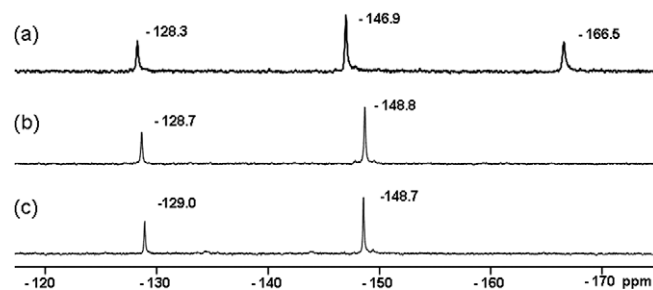

Fig. 11. $^{119}Sn\{^1H\}$ NMR spectra at 298 K of successive additions of phenazine (**2**) to a CD$_2$Cl$_2$ solution of $[n\text{-}Bu_2Sn(\mu\text{-}OH)(H_2O)_{0.5}(\eta^1\text{-}O_3SCF_3)]_2$ (**1**): (a) equimolar mixture (b) reaction conditions (molar ratio = 3:1), and (c) large excess of phenazine (molar ratio = 6:1).

4. Conclusion

Usually, the construction of coordination polymers or metal–organic coordination is based on the association of metal centres with appropriate organic ligands. This contribution supported by solid-state studies as well as IR and $^{119}Sn\{^1H\}$ NMR spectroscopy investigations has exposed an unusual route to the generation of such polymeric edifices, highlighting the opportunity to utilize preformed organometallic complexes as building-blocks in presence of a chemical initiator which promotes the process of polymerisation. Indeed, we have reported the preparation at room temperature of the novel two-dimensional framework, $^2_\infty\{[n\text{-}Bu_2(\mu\text{-}OH)SnOSn(\mu\text{-}\eta^2\text{-}O_3SCF_3)n\text{-}Bu_2]_2[n\text{-}Bu_2(\mu\text{-}OH)SnOSn(\eta^1\text{-}O_3SCF_3)n\text{-}Bu_2]_2\}$ (**3**), from $[n\text{-}Bu_2Sn(\mu\text{-}OH)(H_2O)_{0.5}(\eta^1\text{-}O_3SCF_3)]_2$ (**1**) and phenazine (**2**). In addition, varying the solvent of crystallization, we have shown the conversion of the title compound into the polymorphic structure $^2_\infty\{[n\text{-}Bu_2(\mu\text{-}OH)SnOSn(\mu\text{-}\eta^2\text{-}O_3\text{-}SCF_3)n\text{-}Bu_2]\}$ (**3b**) and we have isolated from the initial reaction two unprecedented structural arrangements for the phenazinium trifluoromethanesulfonate salt, $[C_{12}H_9N_2]^+$ $[CF_3SO_3]^-$ (**4**) and $\{([C_{12}H_9N_2]^+ [CF_3SO_3]^-)_2(C_{12}H_8N_2)\}$ (**5**). We are currently attempting to apply and generalize the reported approach to new examples.

Appendix A. Supplementary material

CCDC 667811, 667812, 667813 and 667814 contain the supplementary crystallographic data for **3**, **3b**, **4** and **5**. These data can be obtained free of charge from The Cambridge Crystallographic Data Centre via www.ccdc.cam.ac.uk/data_request/cif. Supplementary data associated with this article can be found, in the online version, at doi:10.1016/j.jorganchem.2009.03.027.

References

[1] M. Fujita, Y.J. Kwon, S. Washizu, K. Ogura, J. Am. Chem. Soc. 116 (1994) 1151.
[2] O.R. Ewans, H.L. Ngo, W. Lin, J. Am. Chem. Soc. 123 (2001) 10395.
[3] R. Tannenbaum, Chem. Mater. 6 (1994) 550.
[4] T. Sawaki, T. Dewa, Y. Aoyama, J. Am. Chem. Soc. 120 (1998) 8539.
[5] T. Sawaki, Y. Aoyama, J. Am. Chem. Soc. 121 (1999) 4793.
[6] B. Gomez-Lor, E. Gutierrez-Puebla, M. Iglesias, M.A. Monge, C. Ruiz-Valero, Inorg. Chem. 41 (2002) 2429.
[7] L.-X. Dai, Angew. Chem., Int. Ed. 43 (2004) 5726.
[8] Y.M.A. Yamada, Y. Maeda, Y. Uozumi, Org. Lett. 8 (2006) 4259.

[9] F. Bramsen, A.D. Bond, C.J. McKenzie, R.G. Hazell, B. Moubaraki, K.S. Murray, Chem. Eur. J. 11 (2005) 825.
[10] R. Kiyaura, K. Seki, G. Akyama, S. Kitagawa, Angew. Chem., Int. Ed. 42 (2003) 428.
[11] A.R. Millward, O.M. Yaghi, J. Am. Chem. Soc. 127 (2005) 17998.
[12] J.A.R. Navarro, E. Barea, J.M. Salas, N. Masciocchi, S. Galli, A. Sironi, C.O. Ania, J.B. Parra, Inorg. Chem. 45 (2006) 2397.
[13] S.D. Huang, R.-G. Xiong, Polyhedron 16 (1997) 3929.
[14] R. Matsuda, R. Kitaura, S. Kitagawa, Y. Kubota, T.C. Kobayashi, S. Horike, M. Takata, J. Am. Chem. Soc. 126 (2004) 14063.
[15] Y. Kubota, M. Takata, R. Matsuda, R. Kitaura, S. Kitagawa, K. Kato, M. Sakata, T.C. Kobayashi, Angew. Chem., Int. Ed. 44 (2005) 920.
[16] D. Bradshaw, J.B. Claridge, E.J. Cussen, T.J. Prior, M.J. Rosseinsky, Acc. Chem. Res. 38 (2005) 273.
[17] D. Olea, S.S. Alexandre, P. Amo-Ochoa, A. Guijarro, F. de Jesús, J.M. Soler, P.J. de Pablo, F. Zamora, J. Gómez-Herrero, Adv. Mater. 17 (2005) 1761.
[18] C. Janiak, Dalton Trans. (2003) 2781.
[19] A.Y. Robin, K. Fromm, Coord. Chem. Rev. 250 (2006) 2127.
[20] M. Eddaoudi, D.B. Moler, H. Li, B. Chen, T.M. Reineke, M. O'Keeffe, O. Yaghi, Acc. Chem. Res. 34 (2001) 319.
[21] J.D. Ranford, J.J. Vittal, D. Wu, Angew. Chem., Int. Ed. 37 (1998) 1114.
[22] M. Oh, G.B. Carpenter, D.A. Sweigart, Angew. Chem., Int. Ed. 41 (2002) 3650.
[23] M. Oh, G.B. Carpenter, D.A. Sweigart, Chem. Commun. (2002) 2168.
[24] B. Cnerney, P. Jensen, P.E. Kruger, B. Moubraki, K.S. Murray, Cryst. Eng. Commun. 5 (2003) 454.
[25] M. Oh, G.B. Carpenter, D.A. Sweigart, Macromol. Symp. 196 (2003) 101.
[26] J.A. Reingold, S.U. Son, G.B. Carpenter, D.A. Sweigart, J. Inorg. Organomet. Polym. Mat. 16 (2006) 1.
[27] H.D. Selby, B.K. Roland, Z. Zheng, Acc. Chem. Res. 36 (2003) 933.
[28] K. Liang, H.-G. Zheng, Y.-L. Song, Cryst. Growth Des. 7 (2007) 373.
[29] D. Ballivet-Tkatchenko, O. Douteau, S. Stutzmann, Organometallics 19 (2000) 4563.
[30] D. Ballivet-Tkatchenko, R. Burgat, R. Ligabue, L. Plasseraud, D. Poinsot, Appl. Catal. A 255 (2003) 93.
[31] D. Ballivet-Tkatchenko, S. Chambrey, R. Keiski, R. Ligabue, L. Plasseraud, P. Richard, H. Turunen, Catal. Today 115 (2006) 80.
[32] D. Ballivet-Tkatchenko, H. Chermette, L. Plasseraud, O. Walter, Dalton Trans. (2006) 5167.
[33] A. Orita, K. Sakamoto, H. Ikeda, J. Xiang, J. Otera, Chem. Lett. (2001) 40.
[34] H. Lee, J.Y. Bae, O.-S. Kwon, S.J. Kim, S.D. Lee, H.S. Kim, J. Organomet. Chem. 689 (2004) 271.
[35] A. Altomare, G. Cascarano, C. Giacovazzo, A. Guagliardi, J. Appl. Crystallogr. 26 (1993) 343.
[36] G.M. Sheldrick, SHELX-97 (Includes SHELXS-97 and SHELXL-97), Release 97-2. Programs for Crystal Structure Determination, University of Göttingen, Göttingen, Germany, 1998.
[37] L.J. Farrugia, J. Appl. Crystallogr. 32 (1999) 837.
[38] D.H. Johnston, D.F. Shriver, Inorg. Chem. 32 (1993) 1045.
[39] V. Chandrasekhar, S. Nagendran, V. Baskar, Coord. Chem. Rev. 235 (2002) 1.
[40] The term of pseudo-terminal defines a trifluoromethanesulfonate group terminally coordinated to a tin centre of the 1D polymeric chain, but also acting as bridging ligand between two chains through non-coordination intermolecular forces to form the 2D network.
[41] G.A. Lawrance, Chem. Rev. 86 (1986) 17.
[42] J. Beckmann, D. Dakternieks, A. Duthie, F.S. Kuan, Organometallics 22 (2003) 4399.
[43] J. Beckmann, Appl. Organomet. Chem. 19 (2005) 494.
[44] T. Sato, Y. Wakahara, J. Otera, H. Nozaki, Tetrahedron 47 (1991) 9773.
[45] T. Sato, Y. Wakahara, J. Otera, H. Nozaki, Tetrahedron Lett. 31 (1990) 1581.
[46] K. Sakamoto, Y. Hamada, H. Akashi, A. Orita, J. Otera, Organometallics 18 (1999) 3555.
[47] H. Lee, J.Y. Bae, O.S. Kwon, S.J. Kim, S.D. Lee, H.S. Kim, J. Organomet. Chem. 689 (2004) 1816.
[48] D. Ballivet-Tkatchenko, H. Cattey, L. Plasseraud, P. Richard, Acta Crystallogr. E 62 (2006) m2820.
[49] R.-H. Wang, M.-C. Hong, J.-H. Luo, R. Cao, J.-B. Weng, Eur. J. Inorg. (2002) 2082.
[50] S.P. Narula, S. Kaur, R. Shankar, S. Verma, P. Venugopalan, S.K. Sharma, Inorg. Chem. 38 (1999) 4777.
[51] R. García-Zarracino, J. Ramos-Quiñones, H. Höpfl, Inorg. Chem. 42 (2003) 3835.
[52] R. García-Zarracino, H. Höpfl, J. Am. Chem. Soc. 127 (2005) 3120.
[53] V. Chandrasekhar, R. Thirumoorthi, R. Azhakar, Organometallics 26 (2007) 26.
[54] A. Orita, J. Xiang, K. Sakamoto, J. Otera, J. Organomet. Chem. 624 (2001) 287.
[55] D. Braga, F. Grepioni, Chem. Soc. Rev. 29 (2000) 229.
[56] D. Braga, S.L. Giaffreda, F. Grepioni, L. Maini, M. Polito, Coor. Chem. Rev. 250 (2006) 1267.
[57] For a recent review on orthogonal electrostatic interactions between dipoles in structural chemistry and biology. See: R. Paulini, K. Müller, F. Diederich, Angew. Chem., Int. Ed. 44 (2005) 1788.
[58] M. Munkata, T. Kuroda-Sowa, M. Maekawa, A. Honda, S. Kitagawa, J. Chem. Soc., Dalton Trans. (1994) 5525.
[59] C.A. Hunter, J.K.M. Sanders, J. Am. Chem. Soc. 112 (1990) 5525.
[60] C. Janiak, J. Chem. Soc., Dalton Trans. (2000) 3885.
[61] B. Yan, V.O. Golub, A. Lachgar, Inorg. Chim. Acta 359 (2006) 118.
[62] G.A. Davis, J.D. Gresser, P.A. Carapelluci, J. Am. Chem. Soc. 93 (1971) 2179.
[63] V.R. Thalladi, T. Smolka, R. Boese, R. Sustmann, Cryst. Eng. Commun. (2000) 17.
[64] V.R. Thalladi, T. Smolka, A. Gehrke, R. Boese, R. Sustmann, New J. Chem. 24 (2000) 143.
[65] Y.S.J. Veldhuizen, W.J.J. Smeets, N. Veldman, A.L. Spek, C. Faulmann, P. Auban-Senzier, D. Jerome, P.M. Paulus, J.G. Haasnoot, J. Reedijk, Inorg. Chem. 36 (1997) 4930.
[66] K. Gotoh, T. Asaji, H. Ishida, Acta Crystallogr. C 63 (2007) o17.
[67] L. Sieron, Acta Crystallogr. E 63 (2007) o250.
[68] V. Chandrasekhar, P. Singh, K. Gopal, Organometallics 26 (2007) 2833.
[69] T. Yano, K. Nakashima, J. Otera, R. Okawara, Organometallics 4 (1985) 1501.
[70] J. Beckmann, D. Dakternieks, A. Duthie, K. Jurkschat, M. Mehring, C. Mitchell, M. Schürmann, Eur. J. Inorg. Chem. (2003) 4356.
[71] D. Ballivet-Tkatchenko, R. Burgat, S. Chambrey, L. Plasseraud, P. Richard, J. Organomet. Chem. 691 (2006) 1498.